

## Supporting information

### **Pyroelectric nanoplatform for NIR-II triggered photothermal therapy with pyroelectric dynamic therapy**

*Zhongmin Tang,<sup>a,b</sup> Peiran Zhao,<sup>c</sup> Dalong Ni,<sup>a,b</sup> Yanyan Liu,<sup>c</sup> Meng Zhang,<sup>a,b</sup> Han Wang,<sup>a,b</sup> Hua Zhang,<sup>d</sup> Hongbo Gao,<sup>e</sup> Zhenwei Yao,<sup>d</sup> Wenbo Bu<sup>\*a,c</sup>*

a. Dr. Z. Tang, Dr. D. Ni, Dr. M. Zhang, Dr. H. Wang, Prof. W. Bu

State Key Laboratory of High Performance Ceramics and Superfine Microstructure,  
Shanghai Institute of Ceramics, Chinese Academy of Sciences, Shanghai200050, P.R.  
China. E-mail: wbbu@mail.sic.ac.cn

b. Dr. Z. Tang, Dr. D. Ni, Dr. M. Zhang, Dr. H. Wang

University of Chinese Academy of Sciences, Beijing 100049, P.R. China.

c. Dr. P. Zhao, Dr. Y. Liu Prof. W. Bu

Shanghai Key Laboratory of Green Chemistry and Chemical Processes, School of  
Chemistry and Molecular Engineering, East China Normal University, Shanghai  
200062, P.R. China. E-mail: wbbu@chem.ecnu.edu.cn

d. Dr. H. Zhang, Prof. Z. Yao

Department of Radiology, Huashan Hospital, Fudan University, Shanghai200040, P.R.  
China

e. Dr. H. Gao

Department of Radiology, Fudan University Shanghai Cancer Center, Shanghai  
200032, China.

## 1. Supplementary Methods

**Synthesis of SnSe nanorods.**  $\text{SnCl}_2 \cdot 2\text{H}_2\text{O}$ , oleic acid, oleylamine, Se powder, octadecene and dodecanethiol were bought from Sigma-Aldrich Co., Ltd. Polyvinyl Pyrrolidone and cyclohexane were obtained from J&K Chemicals Co., Ltd. And the absolute ethyl alcohol was bought from Richjoint Co., Ltd., Shanghai. All chemical agents were used directly without any purification. Ultrapure water used throughout the experiments was prepared using ELGA water purification system (PURELAB Classic). Firstly, the  $\text{SnCl}_2 \cdot 2\text{H}_2\text{O}$  (5 mmol) powder was immersed in 150 ml solution containing 50 ml oleic acid, 50 ml oleylamine and 50 ml octadecene with sonification for 30 min and stirred for 1 h at room temperature. Then the temperature of the reaction system was slowly increased to 393 K and kept for 2 h under argon (Ar) atmosphere, and the system was naturally cooling to room temperature to obtain  $\text{SnCl}_2$  precursor. In addition, Se (10 mmol) powder was immersed in 30 ml solution including 15 ml oleylamine and 15 ml dodecanethiol and sonicated for 1 h to produce Se precursor. Later, 30 ml  $\text{SnCl}_2$  precursor and 3 ml Se precursor were mixed and stirred for 1 h and the temperature rapidly increased to 473 K and kept for 30 min under Ar atmosphere. After naturally cooling, 20 ml absolute ethyl alcohol was added into the system and stirred for 30 min. Then, the SnSe nanorods were collected by centrifugation and washed three times with cyclohexane and ethanol.

**Surface treatment of SnSe nanorods (SnSe-PVP nanorods).** To transform hydrophobicity of SnSe nanorods into hydrophilicity and improve the biocompatibility, 1 mmol of SnSe nanorods and 1 g PVP40 (average MW 40000) were dispersed in 80 ml

ethanol and sonicated at 333 K for 3 h. After centrifugation with ethanol and water for three times, the SnSe-PVP nanorods were obtained.

**Characterization.** The transmission electron microscopy (TEM) images and corresponding energy dispersive X-ray spectroscopy (EDS) spectra were acquired from the JEM-2100F transmission electron microscope. In addition, the scanning electron microscopy (SEM) images with element mapping scans images were obtained from the S4800 microscope. X-ray photoelectron spectroscopy (XPS) data were monitored on the ESCA lab250 (Thermal Scientific). Besides, X-ray diffraction (XRD) pattern was acquired from the Rigaku D/MAX-2200 PCXRD system (parameters: Cu K $\alpha$ ,  $\lambda = 1.54 \text{ \AA}$ , 25 mA, and 35 kV). The confocal laser scanning microscopy (CLSM) images were recorded from the A1R microscope (Nikon Co.). UV-vis-NIR absorption spectra of SnSe-PVP nanorods were detected using the UV-3600 Shimadzu UV-vis-NIR spectrometer. The quantitative analyses of different elements were determined using the inductively coupled plasma-optical emission spectrometry (ICP-OES, Agilent 725, Agilent Technologies). For the temperature variation and thermal images information, the infrared thermal imaging instrument (FLIR A325SC camera) was employed. The NIR-I and NIR-II lasers were generated from the 808 nm and the 1064 nm large power multimode pump lasers (Shanghai Connect Fiber Optics Co.). PA imaging experiments were conducted on the Vevo LAZR photoacoustic imaging system (Visual-Sonics Co.), which had the parameters: frequency, 21 MHz; PA gain, 40 dB; 2D gain, 10 dB; wavelength, 750 nm.

**Photothermal conversion performance of SnSe-PVP nanorods.** Photothermal

evaluation was monitored through irradiating the cuvette containing SnSe-PVP nanorods solution (300  $\mu\text{L}$ , 25  $\mu\text{g ml}^{-1}$  Se), and the temperature was detected by the camera (FLIRTM A325SC camera, USA) until reaching maxima. And the conversion efficiencies were then calculated, the total energy equation was presented as follows:

$$\sum_i m_i C_{p,i} \frac{dT}{dt} = Q_{in,np} + Q_{in,surr} - Q_{out} \quad (1)$$

where  $m$  and  $C_p$  were the mass and heat capacity of water,  $T$  represented the solution respectively.  $Q_{in,np}$  is the photothermal energy inputted by the SnSe-PVP nanorods, which could be ensured from the following equation:

$$Q_{in,np} = I(1 - 10^{-A_\lambda})\eta \quad (2)$$

Where  $I$  represented the laser power used in the experiment, and the  $A_\lambda$  was the absorbance of SnSe-PVP nanorods at the used wavelength. The  $\eta$  was the photothermal conversion efficiency.

Besides, the  $Q_{in,surr}$  expressed the heat absorbed by the solvent and the container, which was described by:

$$Q_{in,surr} = Q_{Dis} = hS_{buff} \times (T_{max} - T_{Surr})_{buffer} \quad (3)$$

where  $h$  was heat transfer coefficient and  $S_{buff}$  was the surface area of the container.  $T_{max}$  was the maximum steady temperature of the solvent, and  $T_{Surr}$  was the ambient surrounding temperature. The  $Q_{Dis}$  was measured independently to be 0.162 mW (808 nm) and 0.421 (1064nm). In addition,  $Q_{out}$  represented the heat loss to the surrounding environment:

$$Q_{out} = hS \times (T - T_{surr}) \quad (4)$$

Furthermore,  $hS$  could be calculated via determining the rate of temperature decrease

without the laser. Without the light, the equation would be deduced by combining eq.

(4) with eq. (1):

$$\sum_i m_i C_{p,i} \frac{dT}{dt} = -Q_{out} = -hS \times (T - T_{surr}) \quad (5)$$

And  $t$  was expressed as the following equation:

$$t = -\left(\frac{m_{buff} C_{p,buff}}{hS}\right) \ln\left(\frac{T - T_{surr}}{T_{max} - T_{surr}}\right) \quad (6)$$

Where two rate constants were defined as  $\tau_s$

$$\tau_s = \frac{m_{buff} \times C_{p,buff}}{hS} \quad (7)$$

and  $\theta$  expressed

$$\theta = \frac{T - T_{surr}}{T_{max} - T_{surr}} \quad (8)$$

Combining eq. (6), eq. (7) and eq. (8) yields:

$$t = -\tau_s \ln(\theta) \quad (9)$$

To obtain the  $hS$ , the cooling curve were monitored and  $\tau_s$  could be determined.

From the fit lines,  $\tau_s$  of SnSe-PVP nanorods (irradiated by 808 nm) was 144.3 s and  $\tau_s$

of SnSe-PVP nanorods (irradiated by 1064 nm) was 206.4 s. At the maximum steady

temperature, eq. (10) was 0 and the following was deduced

$$Q_{in, np} + Q_{in, surr} = I(1 - 10^{-A\lambda})\eta + Q_{Dis} = Q_{out} = hS(T_{max} - T_{surr}) \quad (10)$$

Thus, the photothermal conversion efficiency of SnSe-PVP nanorods can be calculated

as

$$\eta = \frac{hS(T_{max} - T_{surr}) - Q_{dis}}{I(1 - 10^{-A\lambda})} \quad (11)$$

$I$  was the laser power of 300 mW (808 nm) and 780 mw (1064 nm) used during the

experiment and  $A_{808}$  (1.46)  $A_{1064}$  (1.34) were the absorbance of SnSe-PVP nanorods at

the wavelength of 808 nm and 1064 nm. Moreover, the  $m$  was 0.5 g and the  $C$  was 4.2

J/g. With all the data introduced into the eq. (11), the photothermal conversion efficiency ( $\eta$ ) of SnSe-PVP nanorods using 808 nm and 1064 nm were 37.3% and 20.3% respectively.

**Photo-stability of SnSe-PVP nanorods.** The SnSe-PVP nanorods (50  $\mu\text{g}$  Se in 1 ml) was firstly put in the dialysis bag and then irradiated with 1064 nm laser (1  $\text{W cm}^{-2}$ ) for 5 min. Later, the dialysis bag was put into the beaker with 50 ml water surrounded, and 1 ml solution in the beaker was extracted at different time (1 h, 2 h, 3 h, 6 h, 12 h and 24 h) for the detection of Sn concentration using ICP-OES.

***In vitro* cytotoxicity measurement.** 4T1 mouse breast tumor cell line, BRL rat liver cell line and NRK rat kidney cell line were cultured using the high-glucose DMEM (Gibco, USA), which was supplemented with 10% heat-inactivated fetal bovine serum (FBS), 100  $\text{mg ml}^{-1}$  streptomycin and 100 units  $\text{ml}^{-1}$  penicillin. All the cell lines were obtained from Shanghai Institute of cells, Chinese Academy of Sciences, and cultured at 310 K in humid atmosphere with 5% carbon dioxide. To evaluate the cytotoxicities of SnSe-PVP nanorods for different cell lines, the cells were generally seeded (about  $3 \times 10^3$  cells in 100  $\mu\text{l}$  DMEM each well) in 96-well microplates in sextuplicate, and permitted to adhere for 6 h. Then, the culture medium was replaced with fresh DMEM medium including SnSe-PVP nanorods at Se concentration of 0, 0.78, 1.56, 3.13, 6.25, 12.5, 25, 50  $\mu\text{g ml}^{-1}$  respectively. After further co-incubation for 24 h and 48 h, using FBS-free medium containing 0.6  $\text{mg ml}^{-1}$  3-[4,5-dimethylthiazol-2-yl]-2,5-diphenyltetrazolium bromide (MTT) to replace to previous medium. Later, the solution was replaced by 100  $\mu\text{l}$  dimethyl sulfoxide

(DMSO) and incubation for 4 h. With the help of a microplate reader (Bio-TekELx800, USA), potential cell inhibition of SnSe-PVP nanorods was monitored by comparing the absorbance at the wavelength of 490 nm to the control group (n = 6).

***In vitro* inhibition performance of SnSe-PVP nanorods.** Firstly, 4T1 cells were seeded in 96-well microplates ( $3 \times 10^3$  cells per well in DMEM) at 37 °C in humid atmosphere with 5% CO<sub>2</sub>, and allowed to adhere for 6 h. Then fresh DMEM containing SnSe-PVP nanorods ( $25 \mu\text{g mL}^{-1}$  Se) was added to replace the previous DMEM. After further incubation for 4 h, the culture medium was removed and rinsed for three times using PBS (Runcheng Biotech Co., Ltd., Shanghai), then fresh DMEM medium was added into the microplates. After that treatment, using an 808 or 1064 nm laser at 0, 0.5, 1, 1.5 W cm<sup>-2</sup> power intensities to irradiate the cells for 5 min. Finally, the cells viability was evaluated using a standard MTT assay (n = 6). For further Calcein-AM/PI experiment, 4T1 cells were seeded in 1 ml DMEM with  $2 \times 10^4$  cells in CLSM-exclusive culture disks and allowed to adhere for 6 h. The culture medium was then replaced with four groups: 1ml DMEM without SnSe-PVP nanorods, 1 ml DMEM with  $25 \mu\text{g mL}^{-1}$  Se of SnSe-PVP nanorods, 1 ml DMEM with  $25 \mu\text{g mL}^{-1}$  Se of SnSe-PVP nanorods for following 808 nm laser irradiation for 5 min, 1 ml DMEM with  $25 \mu\text{g mL}^{-1}$  Se of SnSe-PVP nanorods for following 1064 nm laser irradiation for 5 min (all 1 W cm<sup>-2</sup> power intensity). After 4 h co-incubation, the medium was removed and washed for three times using PBS to remove remaining materials and replaced with fresh DMEM medium. Then, corresponding treatments

were conducted for the two groups. After co-incubation for 24 h, all cells were collected and washed with Assay Buffer twice to remove residual trypsin. Then the cell suspension was prepared with  $1 \times$  Assay Buffer ( $2 \times 10^4$  to  $5 \times 10^4$  cells  $\text{ml}^{-1}$ ) and stained with 100  $\mu\text{l}$  staining solution, and incubated at 310 K for 30 min. The live and dead cells were monitored using the confocal laser scanning microscopy.

***In vivo* toxicity.** All the animal experiment procedures were according to the guidelines of the Regional Ethics Committee for Animal Experiments, and the care regulations authorized by the Administrative Committee of Laboratory Animals of East China Normal University. Healthy seven-week old female Kunming mice ( $\sim 20$  g) were bought and raised in the Laboratory Rodent Animal Center of East China Normal University. Firstly, female Kunming mice were setted into three groups (each group had six mice) randomly. After the *i.v.* injection of SnSe-PVP nanorods (a dosage of  $40 \text{ mg Kg}^{-1}$  Se in  $150 \mu\text{l}$ ), the mice were sacrificed in 3 days and 30 days respectively, and major organs (heart, liver, spleen, lung and kidney), blood were collected for detailed pathological studies and biochemistry studies.

**Blood circulation, biodistribution and excretion study of SnSe-PVP nanorods.**

For blood circulation of SnSe-PVP nanorods, the blood was collected from the mice ( $n = 3$ ) at different time and then dissolved in the chloroazotic acid to analyze the concentration of Se using ICP-OES. To determine the biodistribution *in vivo*, major organs (liver, spleen, kidney, heart, lung) from Balb/c mice ( $n = 3$ ) were dissected 24 h after the *i.v.* injection of SnSe-PVP nanorods. Then the organs were dissolved in chloroazotic acid under heating to boiling for 2 h. Later, ICP-OES was used to

monitor Se concentrations. To study the excretion of SnSe-PVP nanorods, mice with SnSe-PVP nanorods ( $40 \text{ mg Kg}^{-1} \text{ Se}$ ) *i.v.* injected were housed in metabolic cages to gather their urine and feces. The urine and feces were then digested by chloroazotic acid and detected by ICP-OES.

***In vitro* and *in vivo* PA imaging.** In the *in vitro* PA imaging, the SnSe-PVP nanorods solution (dispersed in purified water) was irradiated using different wavelengths (from 680 nm to 850 nm) to determine the optimal excitation light wavelength as 750 nm. Then the PA signals of different concentrations (3.13, 6.25, 12.5, 25, 50,  $100 \mu\text{g ml}^{-1}$  Se of SnSe-PVP) solution were recorded to induce a linear relation. The wavelength 750 nm was chosen for following *in vivo* PA imaging experiment, and the tumor-bearing mice were intravenously injected with SnSe-PVP nanorods solution ( $40 \text{ mg Kg}^{-1}$  in  $150 \mu\text{l}$ ) and the PA signals were detected at different time points (30, 60, 120, 180 min).

***In vivo* anti-tumor performance using NIR-II biowindow light.** The *in vivo* PTT with PEDT evaluation was performed on 4T1 bilateral tumor-bearing mice. The therapies for 4T1 tumors were carried out when the tumors volume reached  $100 \text{ mm}^3$ , and the mice were anesthetized before  $1064 \text{ nm}$  ( $1 \text{ W cm}^{-2}$ ) laser irradiation. Recording the weight of mice and tumors volume every three days, and the volume was determined according to the formula:  $V = \text{length} \times \text{width}^2 / 2$ . Furthermore, the tumors tissues of different treatments were dissected 24 h after treatments for further H&E staining for histological analysis. When the volume reached  $1000 \text{ mm}^3$ , all the mice were euthanized complied with animal protocol.

## 2. Supplementary Figures

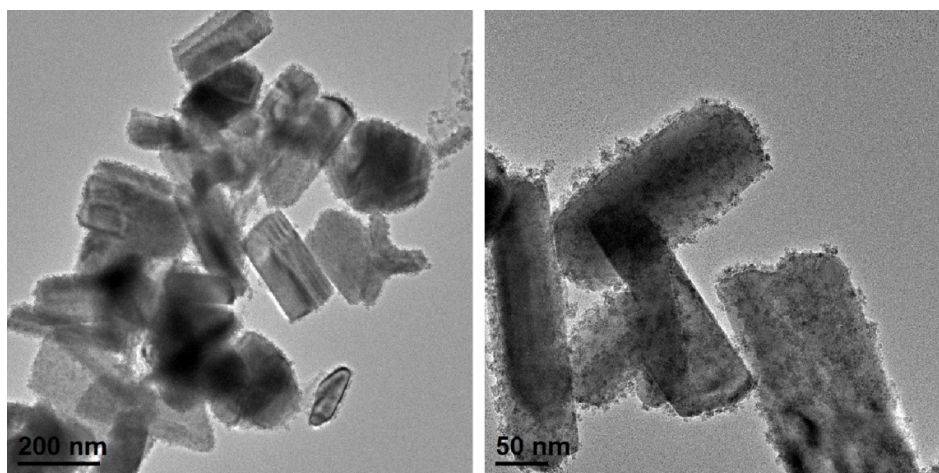


**Figure S1.** Transmission electron microscope (TEM) images of SnSe-PVP nanorods.

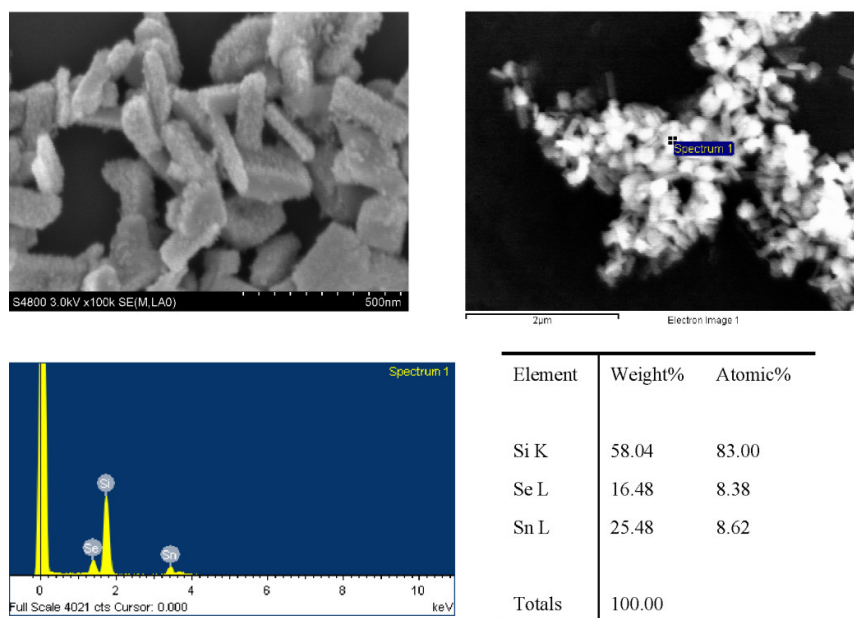


**Figure S2.** Scanning electron microscope (SEM) images, energy Dispersive Spectrum (EDS) and element ratio of SnSe-PVP nanorods.

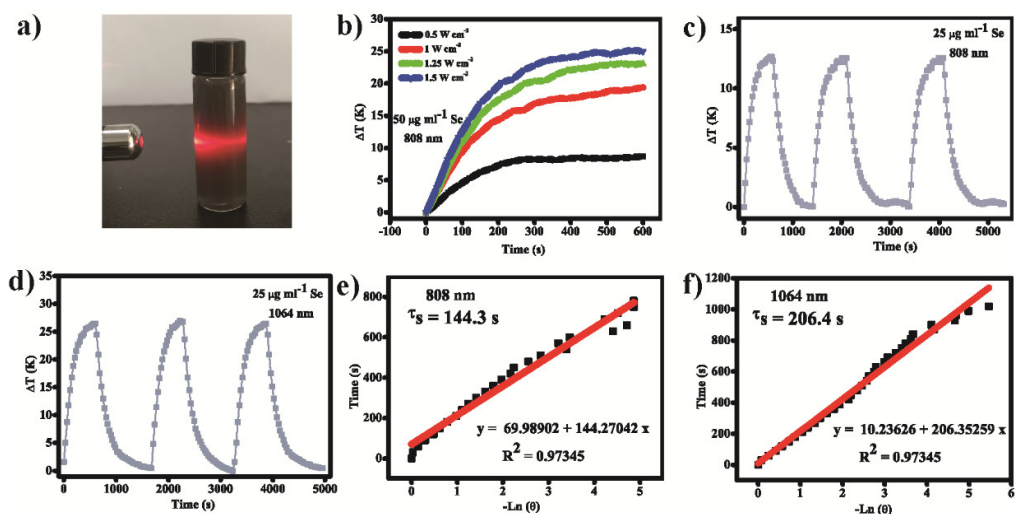


**Figure S3.** (a) Digital photos of SnSe-PVP nanorods solution, revealing strong light absorption ability. (b) Temperature increase of SnSe-PVP nanorods ( $50 \mu\text{g ml}^{-1}$  Se) under irradiation of 808 nm laser at different power intensities ( $0.5, 1, 1.25, 1.5 \text{ W cm}^{-2}$ ). (c,d) Heating and cooling cycles of SnSe-PVP nanorods ( $25 \mu\text{g ml}^{-1}$  Se) under irradiation of 808 nm laser and 1064 nm laser ( $1 \text{ W cm}^{-2}$ ). (e,f) Linear time data vs  $-\ln\theta$  recorded from the cooling period of SnSe-PVP nanorods ( $25 \mu\text{g ml}^{-1}$  Se) under the irradiation of 808 nm and 1064 nm laser ( $1 \text{ W cm}^{-2}$ ) to calculate the  $\tau_s$ .

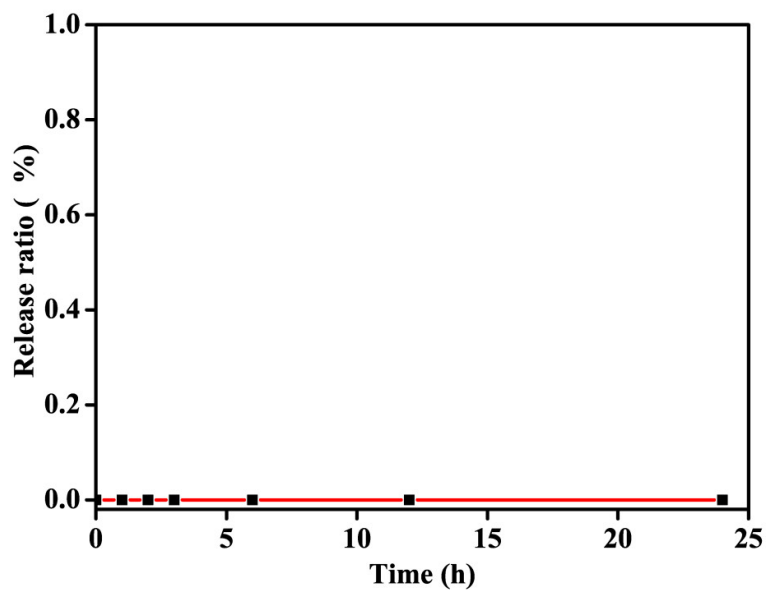


**Figure S4.** The released curve of Sn amount from SnSe-PVP nanorods at different time points (1 h, 2 h, 3 h, 6 h, 12 h and 24 h) after irradiation with 1064 nm laser ( $1 \text{ W cm}^{-2}$ ) for 5 min, which revealed no potential Sn species leakage after laser irradiation.

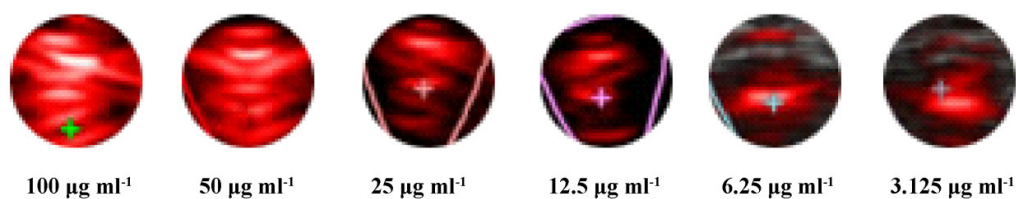


**Figure S5.** PA images of SnSe-PVP nanorods solutions at different concentration of Se, revealing the well PA imaging performance *in vitro*.

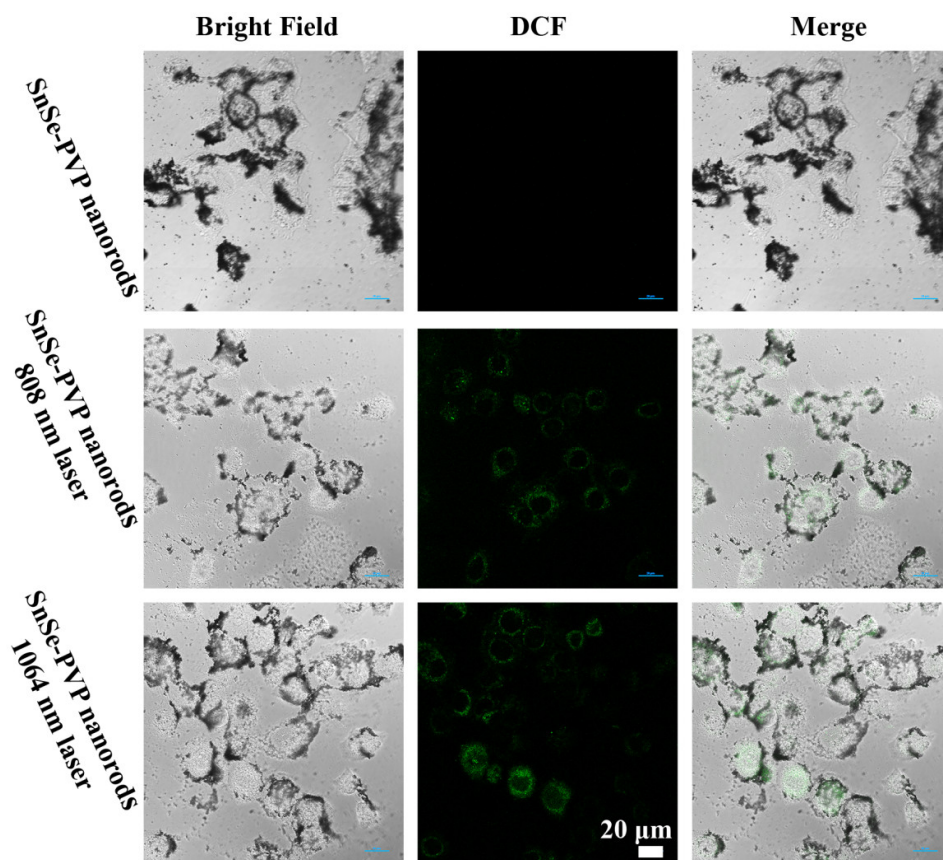


**Figure S6.** Confocal images to reveal the ROS generation ability of PEDT on 4T1 cells in three groups (SnSe-PVP nanorods only, SnSe-PVP nanorods + 808 nm laser, SnSe-PVP nanorods + 1064 nm laser), using 2',7'-dichlorofluorescein diacetate (DCFH-DA) as the probe.

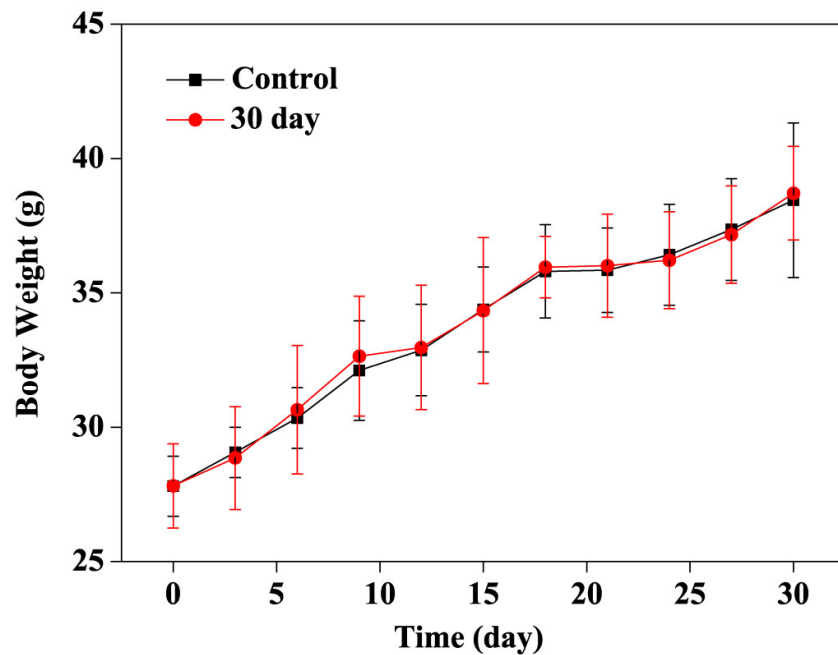


**Figure S7.** Weight change of the control group and the SnSe-PVP nanorods injection group during a month (n = 6, mean  $\pm$  s.d.).

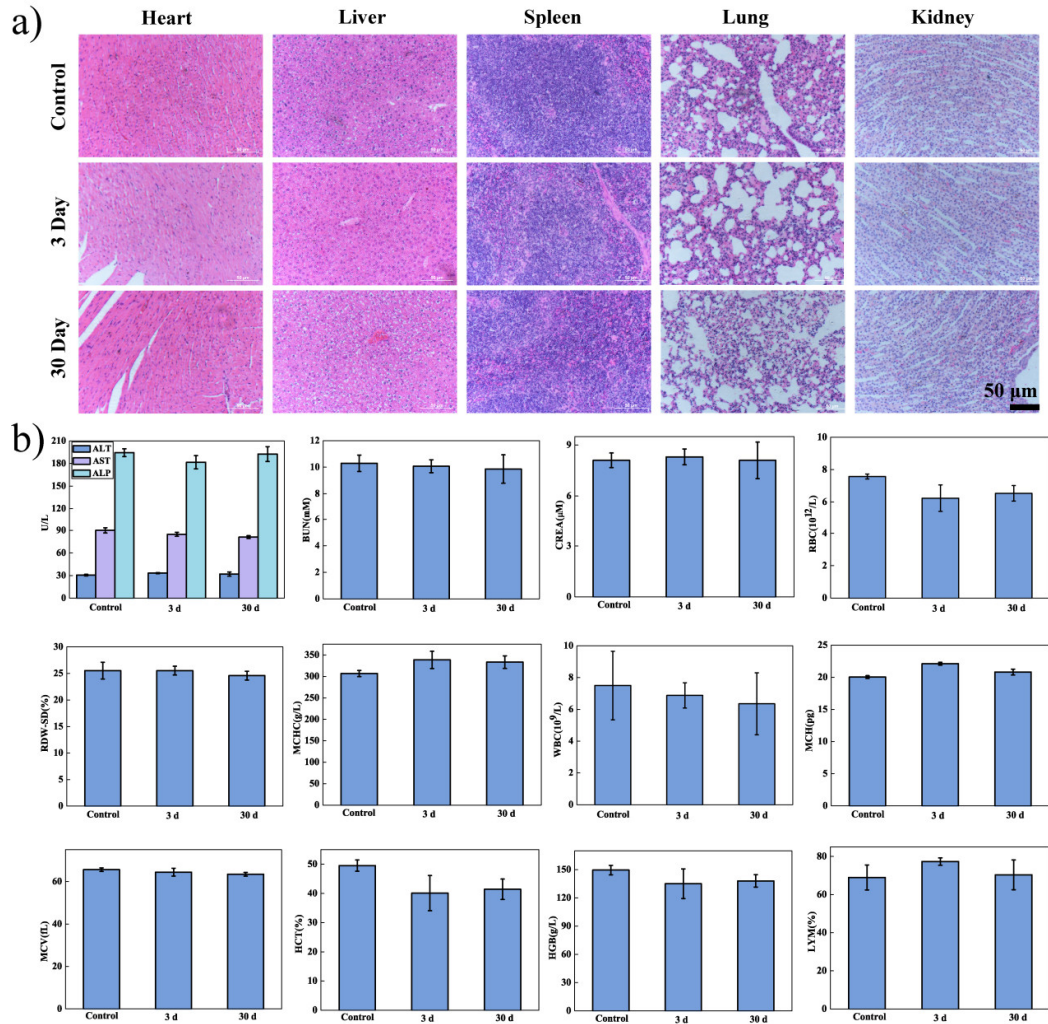


**Figure S8.** (a) Pathological H&E stained pictures of tissue sections from heart, liver, spleen, lung and kidney of the mice of different groups (treated with saline, 3 days after SnSe-PVP injection, 30 days after SnSe-PVP injection). (b) Blood biochemical indexes and hematology parameters of the mice with different treatments (treated with saline, 3 days after SnSe-PVP injection, 30 days after SnSe-PVP injection) (n = 6, mean ± s.d.).

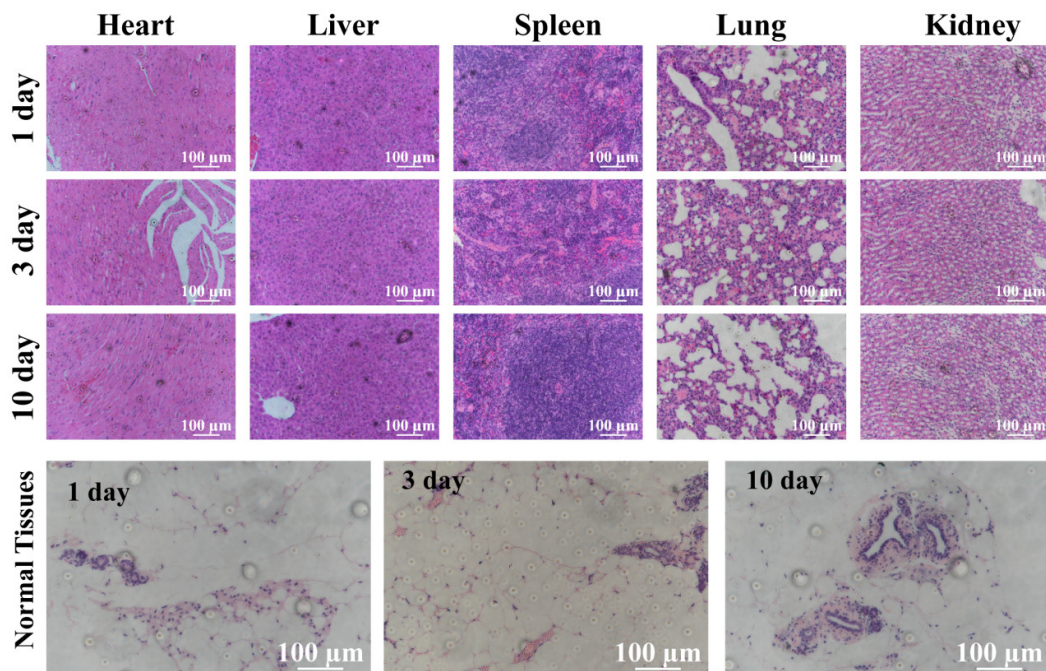


**Figure S9.** Hematoxylin and eosin (H&E) staining results of the main organs (heart, liver, spleen, lung and kidney) and surrounding tissues of tumors of the mice with SnSe-PVP nanorods ( $40 \text{ mg kg}^{-1} \text{ Se}$ ) *i.v.* injected, which were dissected 1 day, 3 day and 10 day after the  $1064 \text{ nm}$  laser ( $1 \text{ W cm}^{-2}$ ) irradiation

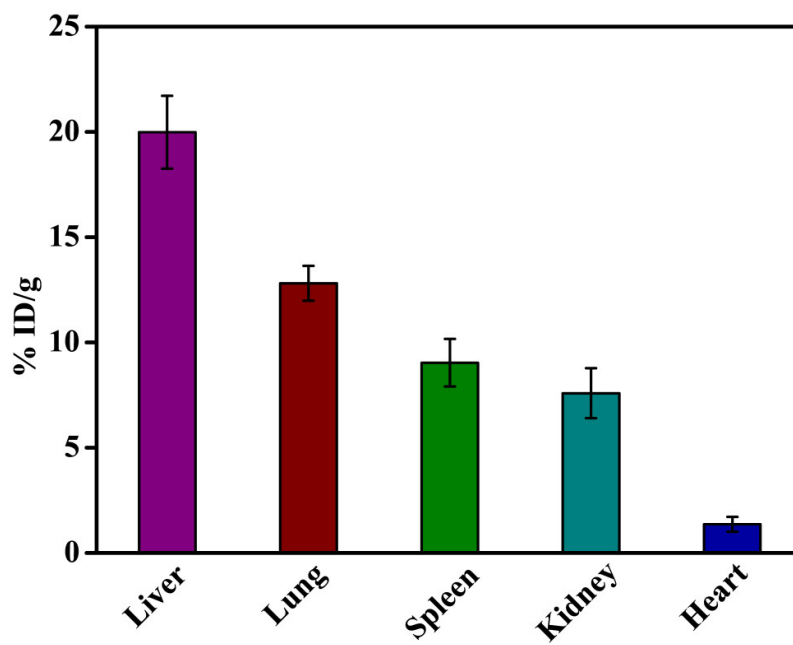


**Figure S10.** Biodistribution of SnSe-PVP nanorods in tumor-bearing mice 24 h after

*i.v.* injection of SnSe-PVP nanorods ( $40 \text{ mg kg}^{-1} \text{ Se}$ ).

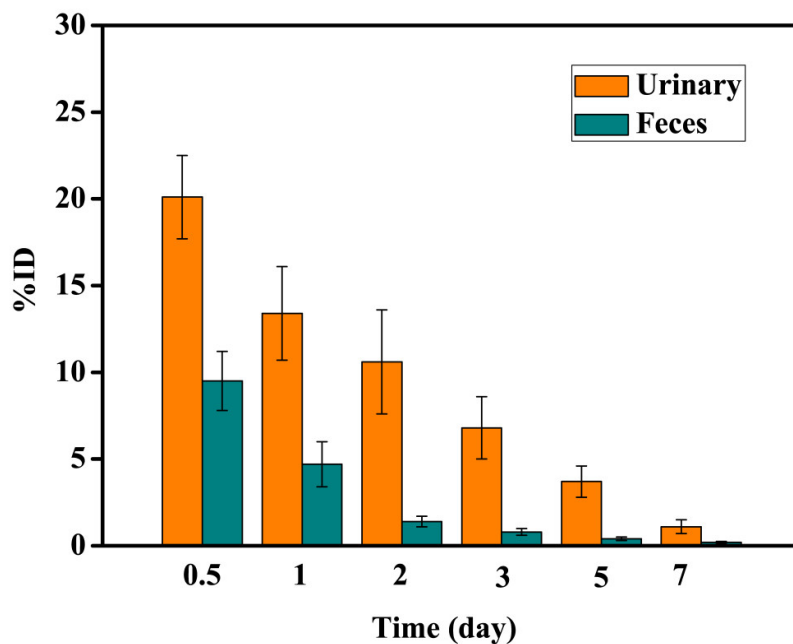


**Figure S11.** The excretion results of Se in healthy mice at different time (0.5 day, 1 day, 2 day, 3 day, 5 day and 7 day) after *i.v.* injection of SnSe-PVP nanorods ( $40 \text{ mg kg}^{-1} \text{ Se}$ ).

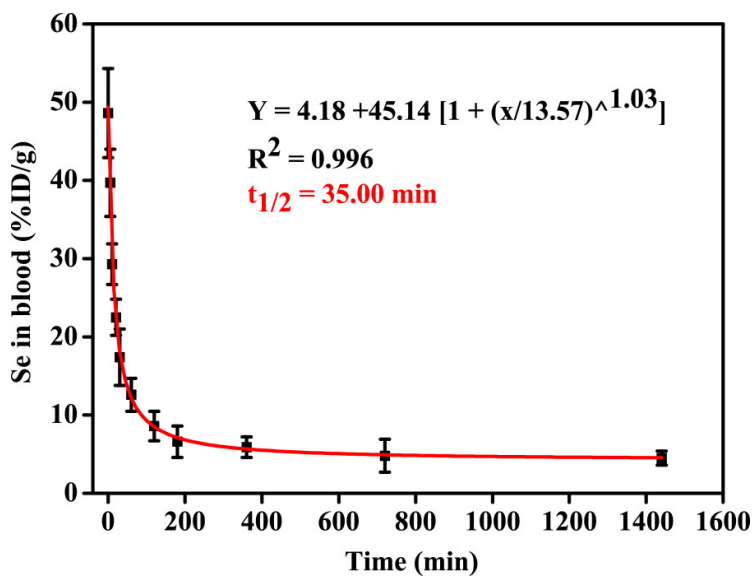


**Figure S12.** The blood circulation of SnSe-PVP nanorods. The pharmacokinetics of SnSe-PVP nanorods followed the one-compartment model.

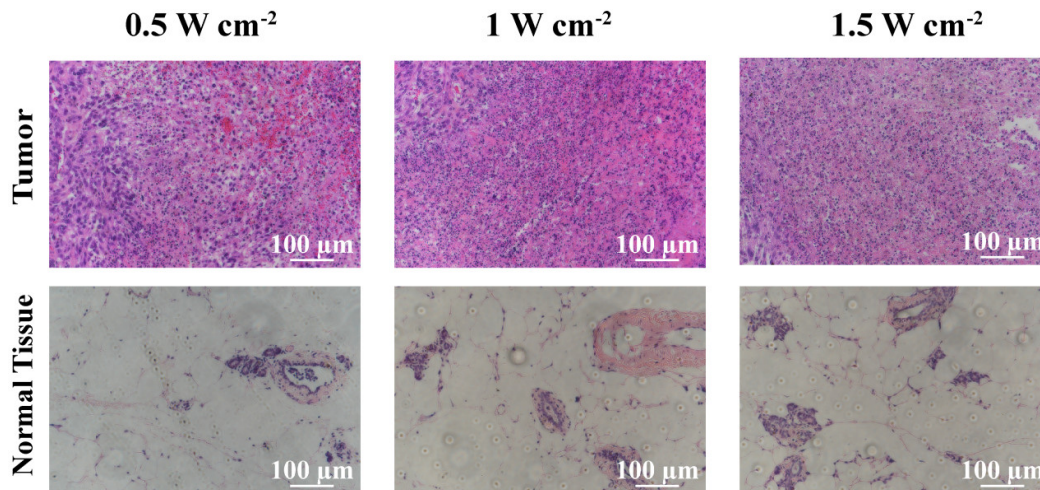


**Figure S13.** H&E staining results of the tumors and surrounding normal tissues of mice with SnSe-PVP nanorods ( $40 \text{ mg kg}^{-1} \text{ Se}$ ) *i.v.* injected, which were dissected 24 h after 1064 nm laser ( $0.5, 1$  and  $1.5 \text{ W cm}^{-2}$ ) irradiation.

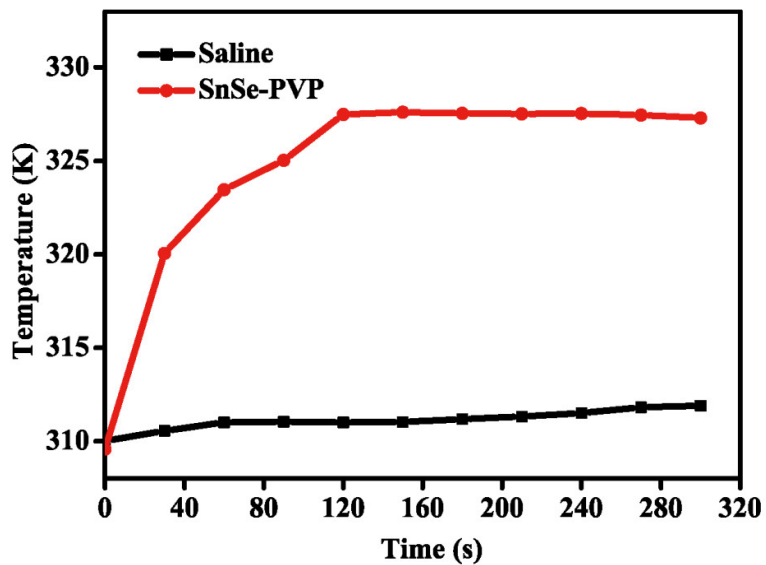


**Figure S14.** Temperature change curves of the mice under irradiation of 1064 nm laser ( $1 \text{ W cm}^{-2}$ ) with saline and SnSe-PVP nanorods injection respectively.

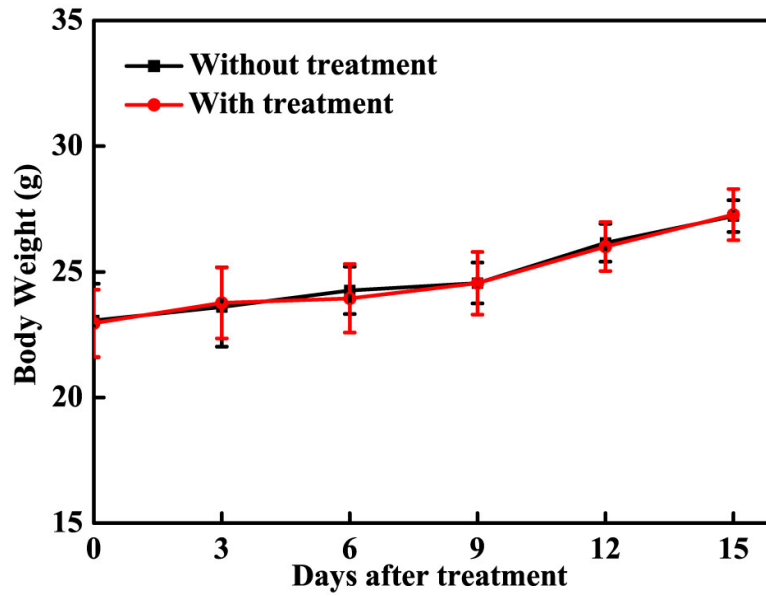


**Figure S15.** Time-course body weight change in 15 days with different treatments (saline injection and SnSe-PVP nanorods injection) (n = 5, mean  $\pm$  s.d.).